

Frequency dependent conductivity of UPd₂Al₃ films

**Martin Dressel, B. P. Gorshunov, Artem V. Pronin, A. A. Mukhin,
Franz Mayr, A. Seeger, Peter Lunkenheimer, Alois Loidl, M. Jourdan,
M. Huth, H. Adrian**

Angaben zur Veröffentlichung / Publication details:

Dressel, Martin, B. P. Gorshunov, Artem V. Pronin, A. A. Mukhin, Franz Mayr, A. Seeger, Peter Lunkenheimer, et al. 1998. "Frequency dependent conductivity of UPd₂Al₃ films." *Physica B* 244: 125-32.
[https://doi.org/10.1016/S0921-4526\(97\)00474-2](https://doi.org/10.1016/S0921-4526(97)00474-2).

Frequency-dependent conductivity of UPd₂Al₃ films

M. Dressel^{a,*}, B.P. Gorshunov^{a,1}, A.V. Pronin^{a,1}, A.A. Mukhin^{a,1}, F. Mayr^a, A. Seeger^a,
P. Lunkenheimer^a, A. Loidl^a, M. Jourdan^b, M. Huth^b, H. Adrian^b

^a *Experimentalphysik V, Universität Augsburg, Universitätsstr. 1, Augsburg 86135, Germany*

^b *Institut für Physik, Universität Mainz, Germany*

Abstract

The transmission of UPd₂Al₃ films was studied ($4\text{ K} < T < 300\text{ K}$) in the frequency range from 4 to 32 cm⁻¹ by using a coherent source interferometer which allows for measuring both, amplitude and phase. In addition we report on radio frequency and optical measurements. Below 20 K the conductivity and dielectric constant show strong deviations from the behavior of a normal metal which cannot simply be explained by a single renormalized Drude model with an enhanced mass and reduced scattering rate. Instead, we find evidence for the opening of a pseudogap with a gap energy of 6 cm⁻¹ and an extremely narrow $\omega = 0$ mode which is responsible for the large DC conductivity.

PACS: 78.20. – e; 71.27. + a

Keywords: Heavy fermions; Magnetic correlations; Thin films; UPd₂Al₃; Submillimeter waves

1. Introduction

Starting with the pioneering work performed by the group of Wachter [1, 2], the electrodynamics of many heavy-fermion metals has been studied intensively for more than 10 years [3–11]. Emerging from a broader Drude behavior above T^* which characterizes normal metals, the contributions of the heavy quasiparticles to the optical conductivity

($T \ll T^*$) are commonly described by the formation of a narrow Drude-like resonance centered at $\omega = 0$ with a scattering rate Γ^* . From spectral weight arguments

$$\int \sigma(\omega) d\omega = \frac{(\omega_p^*)^2}{8} = \frac{\pi n e^2}{2m_b}, \quad (1)$$

with ω_p the plasma frequency and n the carrier density, and assuming [12, 13] an unaffected σ_{DC} , we obtain $\Gamma/\Gamma^* = \omega_p^2/(\omega_p^*)^2 = m^*/m_b$, where m^* denotes the renormalized ‘heavy’ mass, m_b the band-mass, and Γ the unrenormalized relaxation rate.

The heavy-fermion compound UPd₂Al₃ shows coexistence of both superconductivity ($T_c = 2\text{ K}$)

* Corresponding author. E-mail: martin.dressel@physik.uni-augsburg.de.

¹ On leave from Institute of General Physics, Russian Academy of Sciences, Moscow, Russia.

and magnetic ordering ($T_N = 14$ K) [14]. Susceptibility as well as resistivity data indicate $T^* \approx 50$ – 80 K. For $T > 2$ K, i.e. in the normal state below the antiferromagnetic ordering, the specific heat shows a $C_{el}/T \propto T^2$ dependence; the effective mass is estimated as $m^*/m_0 \approx 50$ [14, 15]. While in the compounds UCu_5 and URu_2Si_2 a spin-density-wave develops leading to the opening of a single-particle gap at the Fermi surface which has a distinct influence on the far-infrared optical properties, UPd_2Al_3 shows local moment magnetism and no effect on the infrared optical properties has been observed [10, 11].

In general, the electrodynamic properties of heavy fermions are studied by standard optical reflection measurements down to 20 cm^{-1} , sometimes complemented by surface impedance data from microwave experiments, and a Kramers–Kronig analysis (with the known limitations and uncertainties due to extrapolations) has to be applied to obtain the frequency-dependent conductivity. Avoiding these problems we have studied the transmission through UPd_2Al_3 films in the most interesting frequency range from 4 to 32 cm^{-1} by using a Mach–Zehnder interferometer which allows for measuring the amplitude and the phase. Thus, for the first time we are able to evaluate both independently, the conductivity and the dielectric constant.

2. Experimental Methods and Data Analysis

The highly c -axis oriented (FWHM of the rocking curve is typically 0.5°) thin films of UPd_2Al_3 ($4\text{ mm} \times 8\text{ mm}$) were prepared by independently controlled electron-beam co-evaporation of the constituent elements in a molecular-beam epitaxy system and had a thickness of 1360 \AA . The phase purity and structural quality of the film deposited on a heated (111) oriented $LaAlO_3$ substrate (thickness 1 mm) were investigated by X-ray and reflection high-energy electron diffraction (RHEED); details of the film preparation and characterization are given in Refs. [16, 17]. The high quality of the films is also seen in DC transport data shown in Fig. 1 which are in excellent agreement with results obtained on bulk samples. At $T = 300\text{ K}$

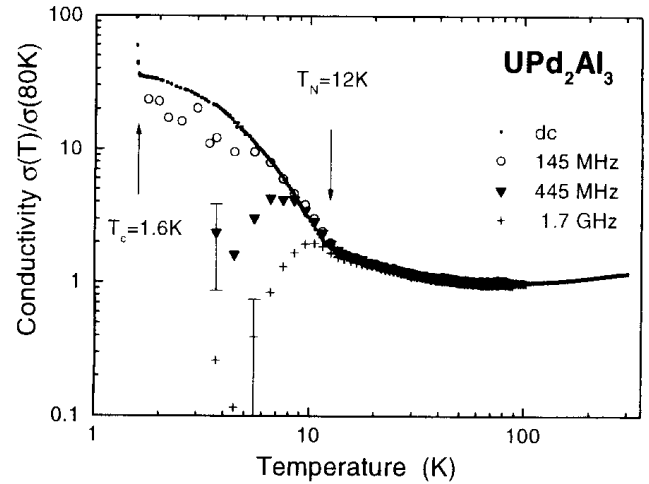


Fig. 1. Temperature dependence of the conductivity of UPd_2Al_3 measured at different frequency ($1\text{ GHz} = 0.033\text{ cm}^{-1}$) as indicated and normalized at $\sigma(T = 80\text{ K})$.

the resistivity is $\rho = 85\text{ }\mu\Omega\text{ cm}$, the Néel temperature is $T_N = 12\text{ K}$; our sample shows a sharp superconducting transition at $T_c = 1.6\text{ K}$.

Transmission measurements on UPd_2Al_3 films were performed in the frequency range from 4 to 32 cm^{-1} utilizing a submillimeter wave spectrometer [18, 19]; the lower-frequency limit is determined by the sample size. Five backward wave oscillators are used as powerful monochromatic, but continuously tunable sources; the beam is guided by polyethylene lenses and mirrors, wire grids act as beam splitters and polarizers; a Golay cell is used for detection. The interferometer is setup in a Mach–Zehnder arrangement which allows for measuring both the amplitude and the phase of the transmitted signal. The sample in the exchange gas of a He-bath cryostat ($3\text{ K} < T < 300\text{ K}$) is positioned in one of the two spectrometer arms; a mirror of the reference arm can be adjusted for destructive interference at each frequency, allowing to determine the optical path length and thus $\varepsilon(\omega)$. The optical parameters of the $LaAlO_3$ substrate are determined by repeating the experiments on a blank substrate.

As an example measured at $T = 20\text{ K}$, the raw data of the transmitted signal and the phase change are displayed in Fig. 2. Using the Fresnel's formulas for a two-layer system [20], the conductivity

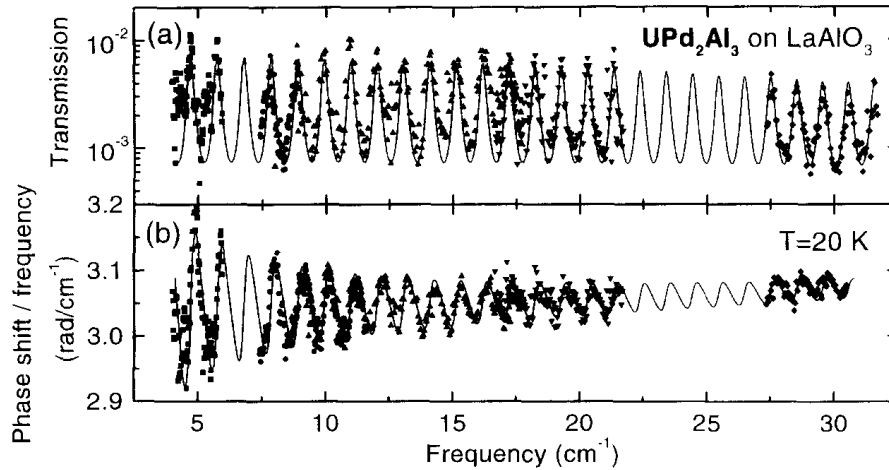


Fig. 2. Raw spectra of the frequency-dependent (a) transmission and (b) phase shift measured at $T = 20$ K through a 136 nm UPd_2Al_3 film on 1 mm LaAlO_3 substrate. The data are obtained using five oscillators ($4\text{--}6\text{ cm}^{-1}$, $7\text{--}12\text{ cm}^{-1}$, $8\text{--}18\text{ cm}^{-1}$, $16\text{--}22\text{ cm}^{-1}$, and $27\text{--}32\text{ cm}^{-1}$). The solid lines represent the description with the Fresnel formulas for a two-layer system.

and dielectric constant of the film are evaluated by simultaneously analyzing the observed transmission amplitude $A(\omega)$ and phase shift $\phi_t(\omega)$ without assuming any particular model (solid line in Fig. 2). Since the description of the interference pattern is most sensitive to the optical properties of the conducting film in the absorption minimum, only data at these frequencies are evaluated further.

To put our results in a broader context, we have also conducted experiments in the radio frequency and microwave range and in the far-infrared spectral range. Four-point resistivity measurements up to 1 MHz performed with an HP 4284A LCR meter give results similar to DC experiments obtained by lock-in technique (113 Hz). Using an HP 4291A impedance analyzer and an HP 8510C network analyzer, high-frequency experiments up to 20 GHz were performed by terminating a coaxial line by the sample. Here the contacts and the geometrical inductance of the sample contribute to the measured results and a proper correction of the data has to be performed; the frequency dependence of the conductivity $\sigma(T)$ can be seen in Fig. 1 (note: $1\text{ GHz} = 0.033\text{ cm}^{-1}$). Measurements of the optical reflection off UPd_2Al_3 films have been performed in an infrared Fourier transform interferometer (Bruker IFS 113v) in the spectral

range from 20 to 600 cm^{-1} down to $T = 3\text{ K}$; the results are in accord with experiments performed on polycrystalline bulk samples and single crystals [10, 11].

3. Results

The temperature dependences of the resistivity $\rho(T) = 1/\sigma(T)$ and of the dielectric constant $\epsilon(T)$ obtained at $\omega/(2\pi c) = 9$ and 30 cm^{-1} are displayed in Fig. 3. From room temperature down to $T = 25\text{ K}$ the electrodynamic response is frequency independent within our accuracy; the absolute value of the room temperature conductivity is in good agreement with the DC results. With increasing frequency, the drop in resistivity below $T = 20\text{ K}$ becomes smaller; consistently the strong temperature dependence of the dielectric constant $\epsilon(T)$ increases with decreasing frequency. In the far-infrared range (e.g. at $\omega/(2\pi c) = 100\text{ cm}^{-1}$), the resistivity even increases as the temperature is lowered, in agreement with the observations reported in Refs. [10, 11]. In Fig. 4, the so-obtained conductivity and dielectric constant is shown as a function of frequency for $T = 4, 10,$ and 25 K for example. By using the simplest model possible, consisting of one Drude term and a single harmonic

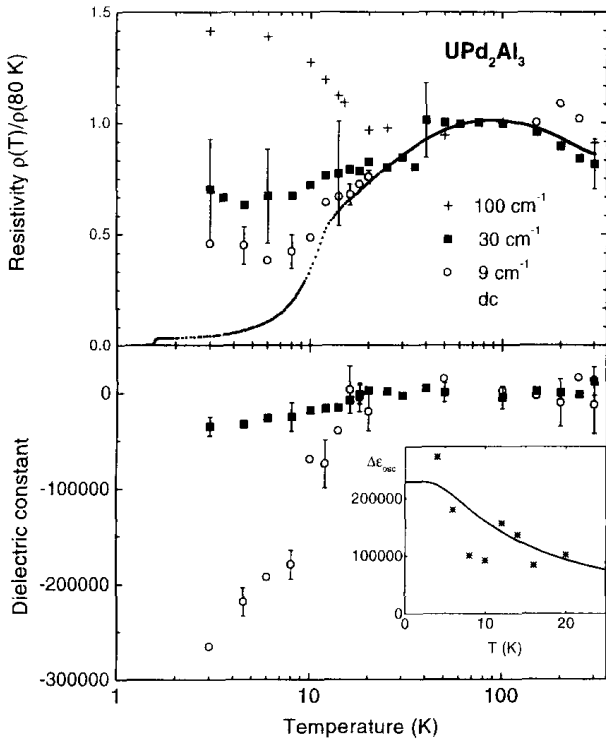


Fig. 3. (a) Temperature dependence of the resistivity of UPd_2Al_3 measured at different frequency as indicated and normalized at the values at $T = 80$ K; (b) temperature dependence of the dielectric constant at $\omega/(2\pi c) = 9$ and 30 cm^{-1} . The inset shows the temperature dependence of the dielectric constant attributed to the finite-energy mode $\Delta\epsilon_{\text{osc}}$.

oscillator [20],

$$\begin{aligned} \epsilon(\omega) + i \frac{4\pi}{\omega} \sigma(\omega) \\ = 1 - \frac{(\omega_p^*)^2}{\omega^2 + i\Gamma^*\omega} + \frac{\omega_{p0}^2}{\omega_0^2 - \omega^2 - i\Gamma_0\omega}, \end{aligned} \quad (2)$$

the frequency dependence of both parameters $\sigma(\omega)$ and $\epsilon(\omega)$ can be well described at each temperature. Here ω_p^* and Γ^* refer to the plasma frequency and scattering rate of the Drude term, respectively; the Lorentz oscillator is characterized by the center frequency ω_0 , the oscillator strength ω_{p0}^2 and the damping Γ_0 . In particular, the dispersion of $\epsilon(\omega)$ can only be explained by the existence of a finite-frequency mode. This procedure is applied to the results obtained at different temperatures. For clarity reasons only the fits by Eq. (2) are displayed in

Fig. 5. Above $T \approx 25$ K, the data for frequencies up to 40 cm^{-1} can be described with a simple Drude model. For an analysis of the higher-frequency optical data see Refs. [10, 11].

4. Discussion

Below T_N , the DC resistivity reflects the freezing out of spin-disorder scattering and can be well described by $\rho(T) = \rho_0 + aT^2 + bT^5$, where the second term indicates the electron–electron scattering, the last term refers to the scattering by acoustic magnons [21]. Attempts have also been made [15, 22] to describe the temperature dependence of the resistivity below T_N by an exponential behavior $\rho(T) = \rho_0 + aT^2 + bT[1 + (2k_B T/E_g)] \exp\{-E_g/k_B T\}$ indicating the opening of a gap in the electronic density of states of approximately $E_g/k_B = 40$ K. From tunneling measurements an extremely large gap energy up to 100 cm^{-1} was suggested [23]. A gap in the magnon dispersion should not necessarily show up in the electronic properties like the resistivity or the optical spectra. The existence of a gap in either the electronic density of states or in the magnon spectrum was already opposed by Caspary et al. [21] and finally ruled out on ground of optical measurements [10, 11]. The weak temperature dependence of the high-frequency response may indicate the remains of magnetic scattering at finite energies. However, we are not aware of any theoretical prediction concerning the frequency dependence of the spin scattering. Interestingly, $\rho(T)$ [15] and μSR results [24] give weak indications that the sister compound UNi_2Al_3 undergoes a transition to an itinerant antiferromagnetic phase (spin-density wave) with the opening of a gap at (parts of) the Fermi surface. No optical investigations have been performed at low temperatures $T < T_N$ in the latter compound.

At first, we would like to comment on the low-frequency (1 MHz–20 GHz) results in UPd_2Al_3 . At frequencies $\omega/(2\pi) > 100$ MHz extremely strong dispersion effects occur below 20 K (Fig. 1). These results indicate an extremely narrow $\omega = 0$ mode. However, due to the contact type of measurements these results reveal large uncertainties and further

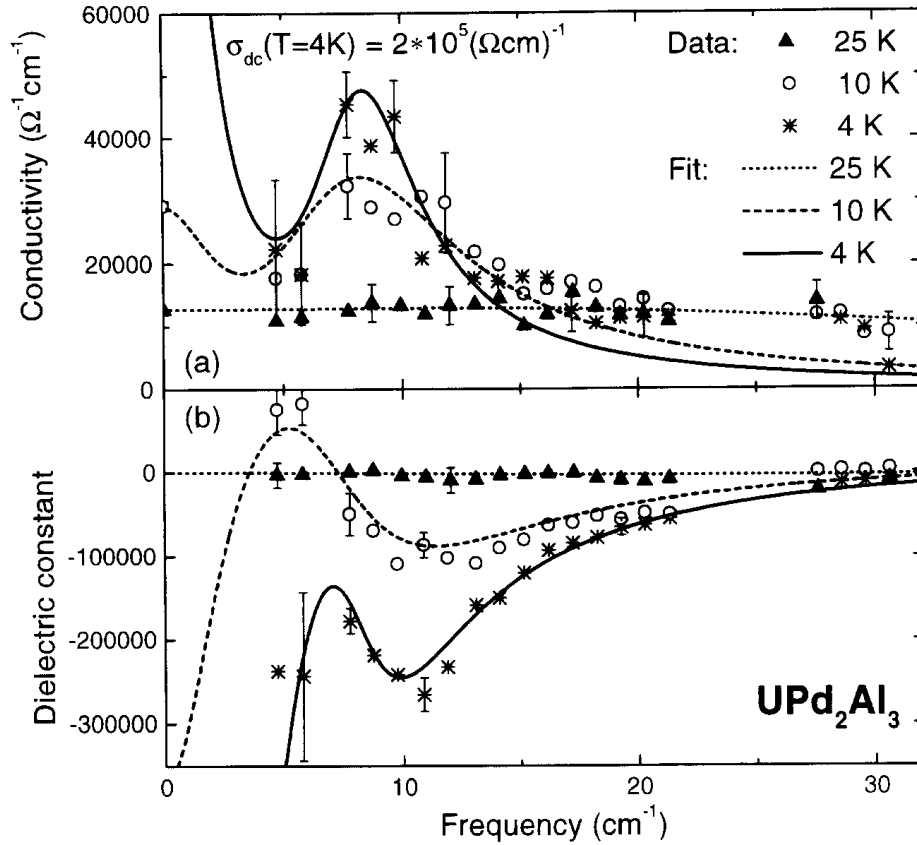


Fig. 4. (a) Frequency-dependent conductivity $\sigma(\omega)$ of UPd_2Al_3 at three different temperatures; (b) corresponding dielectric constant $\epsilon(\omega)$. The symbols are experimental data, the line corresponds to a fit by Eq. (2). Due to the low signal of some of the oscillators (4–6 cm^{-1} and 8–18 cm^{-1}) the large dielectric constant at low temperatures could not be determined reliably in the whole frequency range. Both sets of data are fitted simultaneously with one Drude response and one Lorentz oscillator.

measurements are necessary before final conclusions can be drawn.

We now analyze the behavior below the pseudogap in terms of a renormalized Drude response

$$\hat{\epsilon}(\omega) = 1 + \Delta\epsilon_{\text{osc}} - \frac{(\omega_p^*)^2}{\omega^2 + i\Gamma^*\omega}, \quad (3)$$

where $\Delta\epsilon_{\text{osc}} = \omega_{\text{po}}^2/\omega_0^2$ denotes the contributions of the oscillator to the dielectric constant. Using Eq. (1), we find $\omega_p^*/(2\pi c) \approx 4 \times 10^3 \text{ cm}^{-1}$ at $T = 4 \text{ K}$. Assuming that the total number of charge carriers n remains unchanged and with $\omega_p/(2\pi c) = 4.4 \times 10^4 \text{ cm}^{-1}$ the unrenormalized plasma frequency [10, 11], sum-rule arguments give $m^*/m_b \approx 120$, somewhat larger than the value obtained by thermodynamic methods ($m^*/m_0 = 41\text{--}66$) [14, 15] and

by optical measurements ($m^*/m_b = 85$) [10, 11]. While the scattering rate Γ^* is reduced from 13 cm^{-1} at $T = 20 \text{ K}$ to 1.2 cm^{-1} at 4 K (Fig. 5), the spectral-weight changes only slightly upon cooling leading to a small enhancement of the effective mass m^* which is in accord with the small increase of the Sommerfeld coefficient upon cooling [14]. Based on our present set of data we cannot make a distinct statement on the frequency-dependent renormalization effects leading to a frequency-dependent mass $m^*(\omega)$ and scattering rate $\Gamma^*(\omega)$. This procedure was used to analyze the infrared reflectivity data of the sister compound UNi_2Al_3 above the magnetic ordering temperature [25].

Let us turn to the pseudogap feature. The center frequency ω_0 of the finite-energy mode slightly shifts from 12 to 8 cm^{-1} as the temperature is

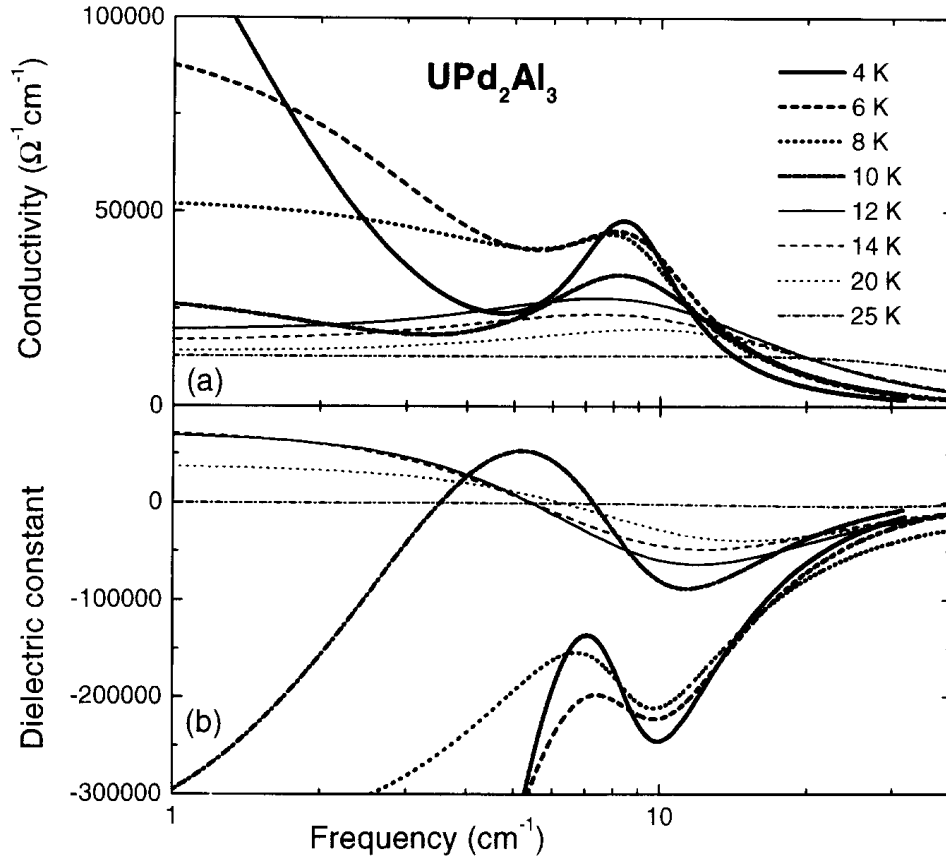


Fig. 5. (a) Frequency-dependent conductivity $\sigma(\omega)$ of UPd_2Al_3 at different temperatures as indicated; (b) corresponding dielectric constant $\epsilon(\omega)$. The fits are obtained by Eq. (2) using one Drude response and one Lorentz oscillator.

lowered from $T = 20$ to 4 K; the damping $\Gamma_0 \approx 6 \text{ cm}^{-1}$ at the lowest temperature. Here the oscillator strength is $\omega_{p0}/(2\pi c) \approx 3500 \text{ cm}^{-1}$ and comparable to the Drude term [26]. One possible explanation of the observed mode is related to the hybridization gap which results from the mixture of the originally localized f-states of uranium ions on a periodic lattice with the band states [27, 28]. The optical conductivity of the periodic Anderson model calculated by Cox and Grewe [29] and by Jarell [30] in infinite-dimensions shows the essential features of our experimental results, however, the energy scale of the model calculations is significantly higher. Theoretically, the gap excitations appear roughly at $2T^*$ while experimentally we observe a peak at about $T^*/5$.

The relative oscillator strength of the direct electron transitions between two peaks of the f-like

density of states can be estimated from our data ($T = 4 \text{ K}$) leading to the spectral weight $\omega_{p0}^2/\omega_p^2 \approx 0.006$. This value lies between the corresponding ratio for f-d transitions (0.3) and f-f atomic transitions (10^{-6}) and thus indicates the mixture of the f and d states. Similar values of the relative oscillator strength were obtained for other heavy-fermion compounds [28]. We note also that the observed oscillator strength decreases with temperature $\omega_{p0}^2(15 \text{ K})/\omega_{p0}^2(4 \text{ K}) \approx 2$, which may be related to the change in the occupation of the split f states. As shown in the inset of Fig. 3 the temperature dependence of the dielectric constant $\Delta\epsilon_{\text{osc}}$ can be well described by $\Delta\epsilon_{\text{osc}} = \Delta\epsilon(0) \tanh\{\hbar\omega_0/(2k_B T)\}$. An alternative explanation of the observed finite-energy mode by crystal-field excitations cannot be completely excluded, although their line widths are large and they are practically

unobservable by inelastic neutron scattering [31]. However, inelastic neutron scattering is only sensitive to magneto-dipole excitations while for the optical conductivity electro-dipole excitations are of importance; these transitions could be responsible for the observed finite-energy mode. In this case we would expect other crystal-field modes at higher frequencies ($\nu > 15 \text{ cm}^{-1}$) which, however, are difficult to detect in reflectivity spectra.

One of the most important questions is the relation between the antiferromagnetic ordering and the finite-energy mode. The fact that we see the gap-like features above T_N up to $T \approx 20 \text{ K}$ does not rule out the connection to the magnetic ordering since an incommensurate phase was observed up to 20 K by neutron diffraction experiments [32]. Assuming only the spin-density-wave character of the antiferromagnetic ordering (i.e. a delocalized magnetic moment of the uranium ions), we would expect for a single-particle gap $E_g/(2\pi\hbar c) = 3.5k_B T_N/(2\pi\hbar c) = 35 \text{ cm}^{-1}$ which is far above the observed pseudogap feature at 6 cm^{-1} . However, it was suggested [21, 33] that two different electronic subsystems coexist in UPd_2Al_3 which originate from the uranium 5f states. One of them is a localized uranium 5f state responsible for the magnetic properties, the other part is delocalized and determines the heavy fermion and superconducting properties. In general, there is some interaction between these states, and we would expect that the antiferromagnetic ordering of the localized magnetic moments affects the heavy-quasiparticle spectrum and the density of states, finally leading to the appearance of pseudogap as observed in our spectra of the conductivity and the dielectric constant. However, the nature of this finite-energy excitation in the low-frequency spectra of UPd_2Al_3 is not clear yet and requires more detailed theoretical and experimental investigations.

Recently, millimeter wave experiments on UPt_3 [34] which indicate a peak in the conductivity at 6 cm^{-1} for temperatures below 5 K gave evidence for a similar scenario. While the finite-energy excitations occur at comparable frequency in UPd_2Al_3 and UPt_3 , the energy scale of the magnetic ordering is different: $T_N \approx 12 \text{ K}$ in UPd_2Al_3 while magnetic correlations are found in UPt_3 only below 5 K [35]. It was argued [34] that the opening of

a pseudogap is a general feature of the heavy-fermion materials probably related to magnetic correlations. Certainly, the interplay between the single-particle character and many-body correlation effects are important for the understanding of the low-energy excitation spectrum.

5. Conclusions

In conclusion, the complex electrodynamic response of UPd_2Al_3 in the energy range below 20 cm^{-1} exhibits a behavior at low temperatures ($T \leq 20 \text{ K}$) which cannot be explained within the simple picture of a renormalized Fermi liquid. Besides an extremely narrow ($\Gamma^* \approx 1 \text{ cm}^{-1}$) Drude-like response we observe a pseudogap with a gap energy of about 6 cm^{-1} . We argue that this feature cannot be related to a single-particle excitation but may be an indication of a low density of states due to electronic correlations.

Acknowledgements

We thank A. Schwartz and G. Grüner for the support during the far-infrared measurements at UCLA and for helpful discussions. The German-Russian scientific cooperation was supported by Deutsche Forschungsgemeinschaft and the Russian Foundation for Basic Research (Grant No. 96-02-17350). Part of the work was supported by the Deutsche Forschungsgemeinschaft through Sonderforschungsbereich 252 Darmstadt/Frankfurt/Mainz.

References

- [1] F. Marabelli, G. Travaglini, P. Wachter, *Solid State Commun.* 59 (1986) 381.
- [2] F. Marabelli, P. Wachter, J.J.M. Franse, *J. Magn. Mater.* 62 (1986) 287.
- [3] B.C. Webb, A.J. Sievers, T. Mihalisin, *Phys. Rev. Lett.* 57 (1986) 1951.
- [4] P.E. Sulewski, A.J. Sievers, M.B. Maple, M.S. Torikachvili, J.L. Smith, Z. Fisk, *Phys. Rev. B* 38 (1988) 5338.
- [5] F. Marabelli, P. Wachter, E. Walker, *Solid State Commun.* 67 (1988) 931.

- [6] F. Marabelli, P. Wachter, *Phys. Rev. B* 42 (1990) 3307.
- [7] F. Marabelli, P. Wachter, *Phys. B* 163 (1990) 224.
- [8] A.W. Awasthi, W. Beyerman, J.P. Carini, G. Grüner, *Phys. Rev. B* 39 (1989) 2377.
- [9] A.M. Awasthi, L. Degiorgi, G. Grüner, Y. Dalichaouch, M.B. Maple, *Phys. Rev. B* 48 (1993) 10692.
- [10] L. Degiorgi, M. Dressel, G. Grüner, P. Wachter, N. Sato, T. Komatsubara, *Europhys. Lett.* 25 (1994) 311.
- [11] L. Degiorgi, S. Thieme, H.R. Ott, M. Dressel, G. Grüner, Y. Dalichaouch, M.B. Maple, Z. Fisk, C. Geibel, F. Steglich, *Z. Phys. B* 102 (1997) 367.
- [12] H. Fukuyama, in: T. Kasuya, T. Saso (Eds.), *Theory of Heavy Fermions and Valence Fluctuations*, Springer, Berlin, 1985.
- [13] A.J. Millis, P.A. Lee, *Phys. Rev. B* 35 (1987) 3394.
- [14] C. Geibel, C. Schank, S. Thies, C.D. Bredl, A. Böhm, M. Rau, A. Grauel, R. Caspary, R. Hefnerich, U. Ahlheim, G. Weber, F. Steglich, *Z. Phys. B* 84 (1991) 1.
- [15] Y. Dalichaouch, M.C. de Andrade, M.B. Maple, *Phys. Rev. B* 46 (1992) 8671.
- [16] M. Huth, A. Kaldowski, J. Hessert, Th. Steinborn, H. Adrian, *Solid State Commun.* 87 (1993) 1133.
- [17] M. Huth, A. Kaldowski, J. Hessert, C. Heske, H. Adrian, *Physica B* 199 and 200 (1994) 116.
- [18] A.A. Volkov, Yu. G. Goncharov, G.V. Kozlov, S.P. Lebedev, A.M. Prokhorov, *Infrared Phys.* 25 (1985) 369.
- [19] A.A. Volkov, G.V. Kozlov, A.M. Prokhorov, *Infrared Phys.* 29 (1989) 747.
- [20] M. Born, E. Wolf, *Principles of Optics*, 4th ed., Pergamon Press, Oxford, 1980.
- [21] R. Caspary, P. Hellmann, M. Keller, G. Sparn, C. Wassilew, T. Köhler, C. Geibel, C. Schank, F. Steglich, N.E. Phillips, *Phys. Rev. Lett.* 71 (1993) 2146.
- [22] K. Bakker, A. de Visser, L.T. Tai, A.A. Menovsky, J.J.M. Franse, *Solid State Commun.* 86 (1993) 497.
- [23] J. Aarts, A.P. Volodin, A.A. Menovsky, G.J. Nieuwenhuys, J.A. Mydosh, *Europhys. Lett.* 26 (1994) 203.
- [24] Y.J. Uemura, G.M. Luke, *Physica B* 186–188 (1993) 223.
- [25] N. Gao, J.D. Garrett, T. Timusk, H.L. Liu, D.B. Tanner, *Phys. Rev. B* 53 (1996) 2601.
- [26] If the total spectral weight $(\omega_p^*)^2 + \omega_{p0}^2$ is attributed to the heavy electrons, we obtain $m^*/m_b = 68$.
- [27] N. Grewe, F. Steglich, in: *Handbook on the Physics and Chemistry of Rare Earths*, vol. 14, Elsevier, Amsterdam, 1991, p. 343.
- [28] P. Wachter, in: *Handbook on the Physics and Chemistry of Rare Earths*, vol. 19, Elsevier, Amsterdam, 1994, p. 177.
- [29] D.L. Cox, N. Grewe, *Z. Phys. B* 71 (1988) 321.
- [30] M. Jarrell, *Phys. Rev. B* 51 (1995) 7429.
- [31] A. Krimmel, A. Loidl, C. Geibel, F. Steglich, *J. Phys.: Condens. Matter* 8 (1996) 1677.
- [32] A. Krimmel, P. Fischer, B. Roessli, H. Maletta, C. Geibel, C. Schank, A. Grauel, A. Loidl, F. Steglich, *Z. Phys. B* 86 (1992) 161.
- [33] R. Feyerherm, A. Amato, F.N. Gyax, A. Schenck, C. Geibel, F. Steglich, N. Sato, T. Komatsubara, *Phys. Rev. Lett.* 73 (1994) 1849.
- [34] S. Donovan, A. Schwartz, G. Grüner, *Phys. Rev. Lett.* 79 (1997) 1401.
- [35] J.K. Kjems, C. Broholm, *J. Magn. Magn. Mater.* 76 (1988) 371.